

1 **CONTRIBUTION OF REMOTE SENSING TO THE IDENTIFICATION OF**  
2 **GROUNDWATER RESOURCES IN MAYO-DALLAH DEPARTMENT, SOUTH-**  
3 **WESTERN CHAD**

4  
5 **Abstract:** Located in south-western Chad, the Department of Mayo-Dallah has a problem of  
6 access to groundwater in terms of quantity due to the complexity of the area (basement). The  
7 aim of this study is to extract the lineaments of the Mayo-Dallah Department using remote  
8 sensing to identify potential groundwater resources. To achieve this, a satellite image (Radar  
9 Sentinel 1-C) was downloaded and subjected to various processing operations. A total of 7193  
10 lineaments were extracted, with lengths ranging from 0.30 to 3Km. 96.7% of the lineaments  
11 are small, less than 1Km. Lineaments of 1 to 3Km considered to be major represent 3.29%.  
12 The distribution of major lineaments on the directional rosette reveals two main directions E-  
13 W and N-S and secondary directions SE-NW, ESE-WNW and NE-SW. The lineament  
14 density map shows that the southern and western parts of the study area have good lineament  
15 density. These areas have a high water potential and could influence recharge.

16 **Keywords:** Chad, groundwater resources, basement, remote sensing, lineaments, Mayo-  
17 Dallah.

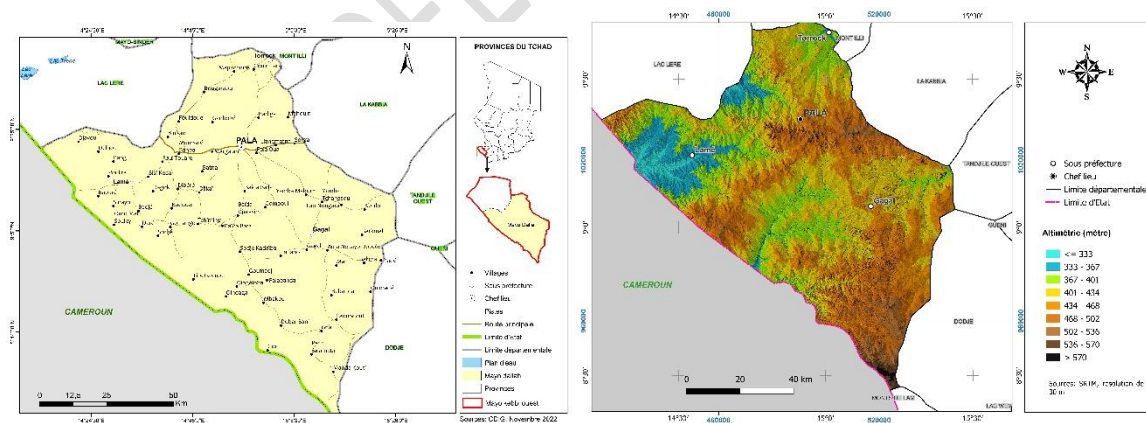
18  
19  
20  
21  
22  
23  
24  
25  
26  
27  
28  
29  
30  
31 **1 - Introduction**

32 Groundwater resources are of vital importance to human life. In developing countries,  
33 they are the first choice for supplying drinking water to the population, due to their good  
34 quality. However, access to these resources is problematic in basement environments. Yet  
35 fractured basement aquifers are excellent groundwater reservoirs (Jourda et al., 2006). The  
36 Department of Mayo-Dallah, the subject of the present study, is characterized in this context.

37 The Department of Mayo-Dallah in south-western Chad belongs to the Sudano-  
 38 Guinean climate zone. It receives an average of 1,000 m of annual rainfall. Despite this  
 39 rainfall, the area suffers from water problems. Borehole flow rates are often low, and the  
 40 failure rate is high. It has been observed that in the dry season, the flow of water in boreholes  
 41 drops considerably and some wells dry up, forcing the population to resort to water of dubious  
 42 quality. According to several authors, this situation can be explained by the poor choice of  
 43 drilling sites and also by the lack of hydrogeological knowledge of the area's aquifers. More  
 44 precise knowledge of fractured aquifers is essential for better location, exploitation and  
 45 sustainable management of their resources (Lasm, 2000), (Koudou et al., 2014). Remote  
 46 sensing is considered an ideal tool in the search for water. It is a preliminary method  
 47 commonly used by hydrogeologists to identify potentially fractured structures considered as  
 48 underground recharge and flow conduits (Mabee et al 2002), (Liee et Gudmundsson, 2002),  
 49 (Gleeson et Novakowski, 2009). With this in mind, it is essential to extract lineaments, as  
 50 their density indicates a high water potential.

51 **2- Presentation of the study area**

52 The Mayo-Dallah Department is located in south-western Chad, in the Mayo-Kebbi  
 53 Ouest Province, between latitudes 8°57' to 10°15'N and longitudes 15°05' to 15°58'E (figure  
 54 1). It covers an area of 4,069 km<sup>2</sup>. It has a Sudano-Guinean climate with two seasons. The dry  
 55 season runs from November to April, and the rainy season from May to October. Annual  
 56 rainfall varies from 900 to 1000mm. Average annual temperatures range from 21.8°C to  
 57 34.9°C. The Department of Mayo-Dallah is home to several temporary watercourses,  
 58 tributaries of the Mayo-kebbi river, with a sinuous morphology imposed by faults (Dournang  
 59 et al., 2021). The topography of the study area is marked by a succession of less accentuated  
 60 reliefs with numerous small hills. Altitudes range from 300 to 500 m, with an average of  
 61 380m above sea level. The lowest points are to the west and slightly to the north-west of the  
 62 study area (figure 1 b).



63  
 64 Figure 1 and 2: Location map and elevation map of Mayo-Dallah Department

65  
 66  
 67 **2.1 - Geological and hydrogeological context**

68 The Mayo-Kebbi West Province consists of a Precambrian basement in the north and  
 69 sedimentary cover formations. The Precambrian basement of Mayo-Kebbi contains three

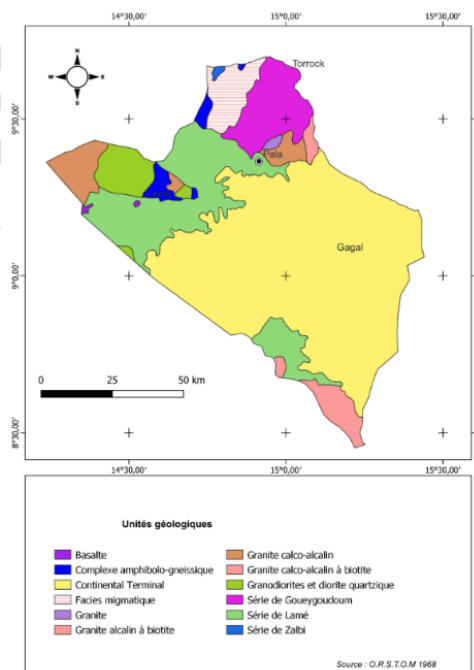
70 groups of rocks : the greenstone belts, the mafic and intermediate complex and the granitoid  
 71 batholith (Mayo-Kebbi batholiths) (Penaye et al., 2005), (Mbagedjé, 2015). These structures  
 72 are all oriented in a NNE-SSW direction. They contain ultrabasic rocks (pyroxenites,  
 73 chloritoschists, talcschists), basic to acidic metaplutonic rocks (gabbros, dioritic gabbros,  
 74 granodiorites and amphiboloschists) and metavolcanosedimentary rocks (amphibolites,  
 75 metabasalts, metadolerites and metagrauwackes) affected by greenschist metamorphism [8].  
 76 The overlying sedimentary formations correspond to the Lamé series (Cretaceous) and the  
 77 Continental Terminal (Doumnang, 2006).

78 Four phases of deformation mark the evolutionary history of the Mayo-Kebbi  
 79 basement. The first two phases are E-W shortening and the third and fourth are represented by  
 80 dextral and senestial detachments respectively (Isseini, 2011).

81 From a hydrogeological point of view, the Mayo-Kebbi basement aquifer is a multi-  
 82 layered aquifer separated by impermeable layers. In the basement, groundwater is located in  
 83 alterites and fracture zones at an average depth of 40m. The static groundwater level depends  
 84 more generally on the strength of the alterites. The median specific flow rate is around 0.18  
 85 m<sup>3</sup>/h/m. There are also deposits with sandy formations, so permeable and capable of ensuring  
 86 borehole productivity. Static level depths are moderate, but flow rates are rather low, of the  
 87 order of 5 m<sup>3</sup>/h at most, with possible dependence on rainfall. Water levels are generally 10  
 88 m deep.

89 In sedimentary formations, aquifers are located in the most permeable layers. Water  
 90 table depths and static levels tend to be moderate, while flow rates are higher and even locally  
 91 interesting (in excess of 15 m<sup>3</sup>/h) (Durand, 2003).

92



93

94 Figure 2: Geological map of the Mayo-Dallah Department

95

### 3- Materials and methods

96

#### 3.1- Materials

97 The material used to achieve our objective is :

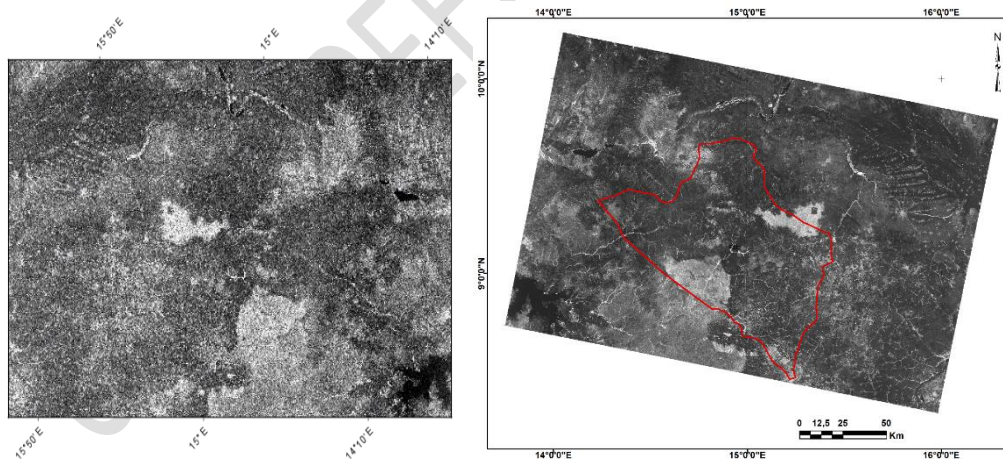
- 98 • The 1:1,500,000 geological map of Chad,
- 99 • Synthetic geological map of the town of Pala,
- 100 • Detailed geological map of Pala,
- 101 • IGN topographic map at 1/200,000 (sheets NC-33-9, NC-33-10, NC-33-11, NC-33-3
- 102 and NC-33-4),
- 103 • Satellite imagery (Radar Sentinel 1-C),
- 104 • Mayo-Kebbi fracturing map extracted from Landsat 7ETM images, scene p184r053,
- 105 Hydrographic network map extracted from SRTM imagery,
- 106 • Borehole data (flow rate and depth).

107 These data are processed on several software packages, namely : SNAP, Arc gis, Geomatica  
108 and Rockwork.

### 109 3.2- Methodology

110 The methodology adopted for this study consists in applying remote sensing processing  
111 methods to extract the lineaments of the study area and to proceed with the control and  
112 validation of these lineaments on the one hand, and to show their relationship with  
113 productivity on the other. To do this, we downloaded an image from the Sentinel 1-C radar  
114 sensor satellites taken on March 16, 2024 from the Copernicus Data Space Ecosystem  
115 website. The satellite data obtained are dual-polarized (HV + VV). Those taken into account  
116 are HV horizontally-vertically polarized. As these are orthorectified images, we directly  
117 applied the Lee sigma 7x7 filter. The filtered image is then exported to Geomatica for  
118 automatic lineament extraction using the Line algorithm.

119 The lineaments obtained are then transferred to Rockwork software for directional analysis.



120

121

122

Figure 3: Satellite images Radar before and after treatment

123

124

## 4- Results

125

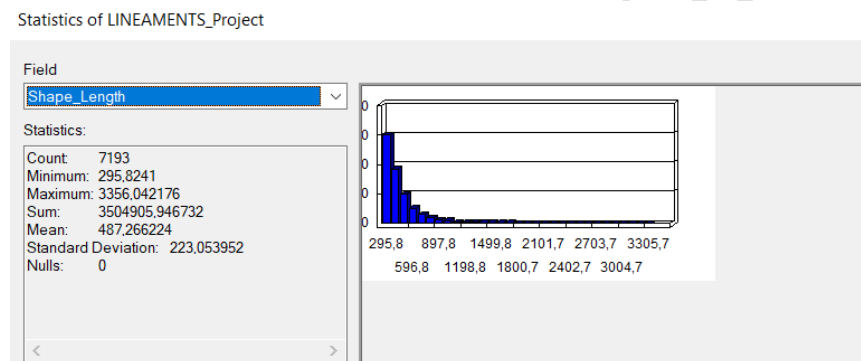
### 4-1 Automatic lineament extraction

126 Application of the LINE modulus algorithm extracted 7193 lineaments with sizes  
127 ranging from 295m to 3000m. Smaller lineaments (less than 1m) are more numerous (figure  
128 4). They account for 96.7% of the total, while lineaments between 1 and 3m account for  
129 3.29%. The latter are considered to be the major lineaments.

130 The distribution of lineaments on the directional rosette is fairly homogeneous. The  
131 frequencies in number and cumulative length are similar. No family exceeds 10% in number  
132 or cumulative length. The N-S and E-W families stand out from the others, with a percentage  
133 in number and cumulative length close to 4%. These are the E-W direction (N80° to 100°)  
134 and the N-S direction (N170° to 180°) (figure 8). These are followed by N160°-170°, N140°-  
135 150°, N0°-20°, N70°-80° with almost 3%. The N40-60° and N110-130° directions are poorly  
136 represented. We can classify these groups into 5 families: N-S (N0-20°, N160-170), SE-NW  
137 (140-150°), ESE-WNW (110-130°), E-W (80-100°), NE-SW (40-60°).

138

139



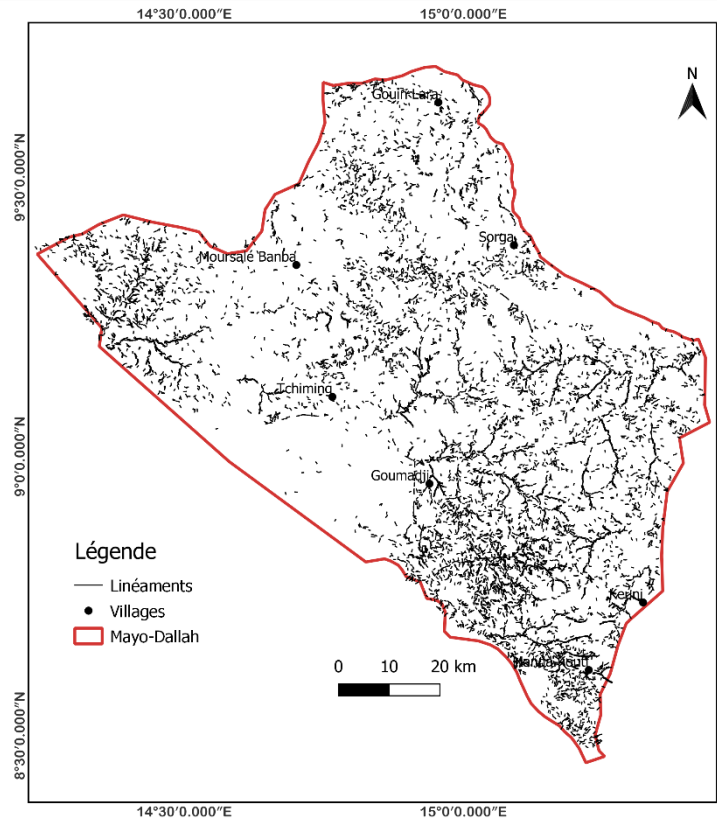
140

141

142

143

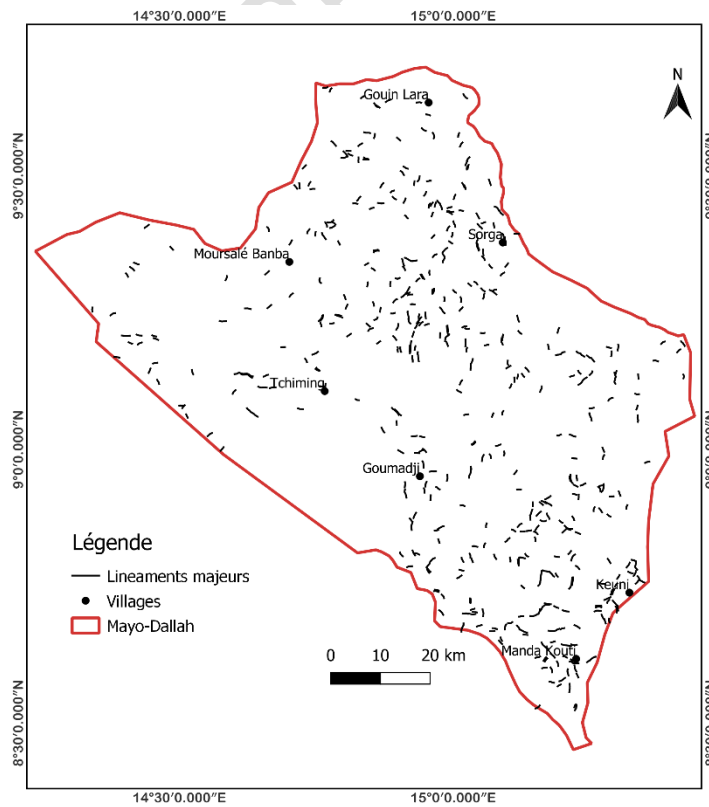
Figure 4: Lineament length frequency histogram



144

145

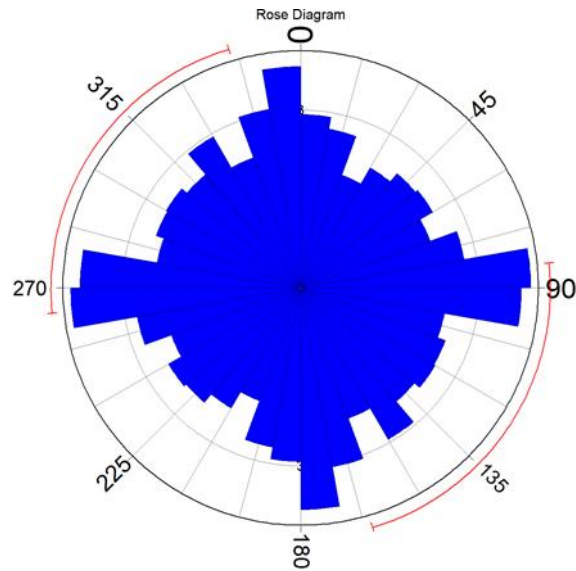
Figure 5: Lineament map of Mayo-Dallah Department



146

147

Figure 6: Map of major lineaments in the Department of Mayo-Dallah



148

149 Figure 7: Directional rosette of the lineaments in the Department of Mayo-Dallah

150

151

### 5- Lineament control and validation

152

153

154

155

156

157

158

159

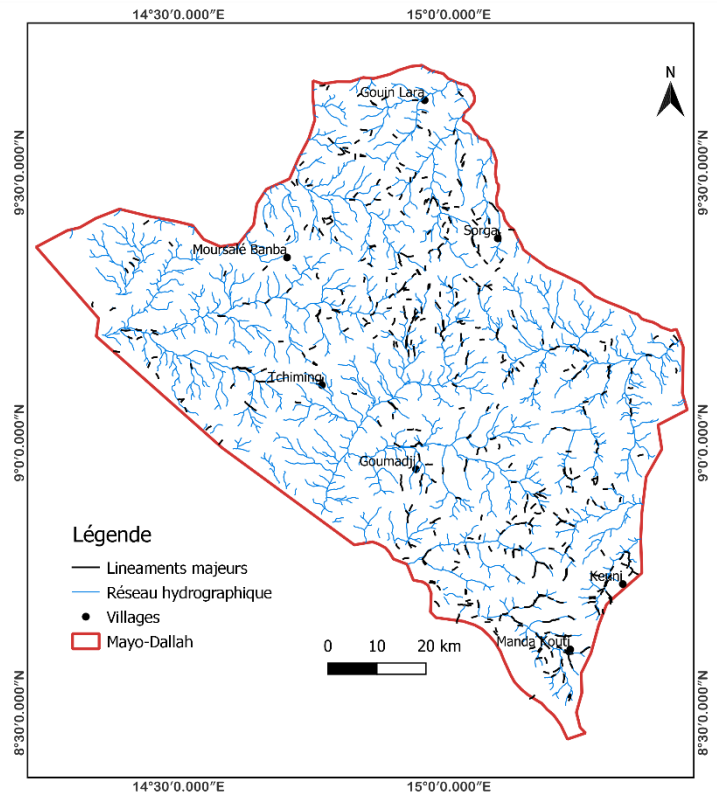
160

161

162

163

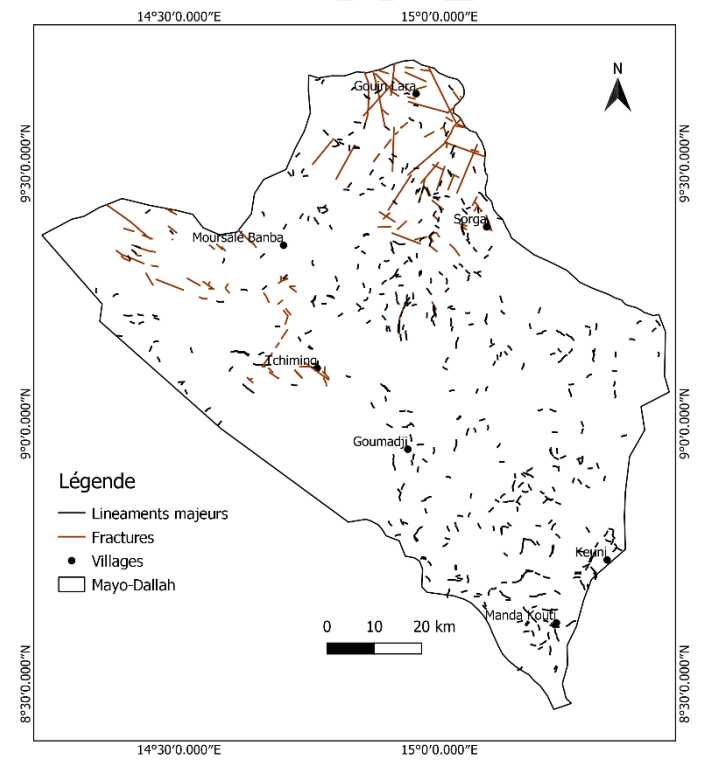
Validation enables us to check the reliability of the method used and to assign fracture values to the lineaments obtained. This stage is based on superimposing the major lineaments on the geoscientific data (hydrographic network, fracturing map and high-flow boreholes). By superimposing the lineaments on the hydrographic network of the study area, illustrated in figure 8, we can see that the lineaments follow the watercourses, which seems logical since, according to (Doumnang et al., 2021), the morphology of the watercourses in the Mayo-Kebbi is imposed by the faults. Figure 9 shows a correspondence of more than 50% between the lineaments and the fractures identified, although not all fractures were found in the field due to the poor outcrop in the study area mentioned by previous authors (Penaye et al., 2005), (Isseini, 2011). This result leads to the conclusion that the lineaments in the study area are of tectonic origin.



164

165

Figure 8: Map of lineaments and hydrographic network



166

167

Figure 9: Map of major lineaments and fractures in the Department of Mayo-Dallah

168

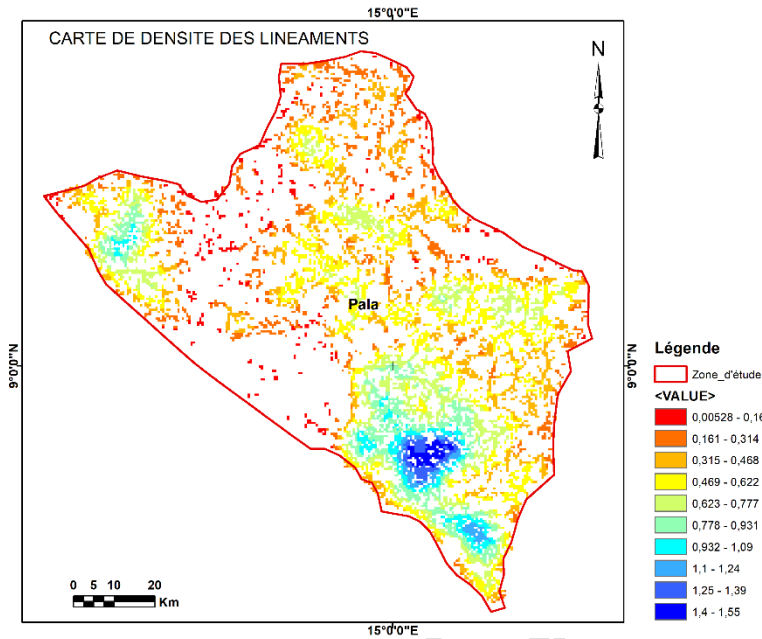
169



170

## 6- Lineament density

171 Density calculates the frequency of lineaments per unit area. The density map shows the  
172 concentration of lineaments per unit area and provides an indication of water potential. Figure  
173 10 shows that the study area is weakly fractured. However, there is good density to the south  
174 and west of the study area.



175

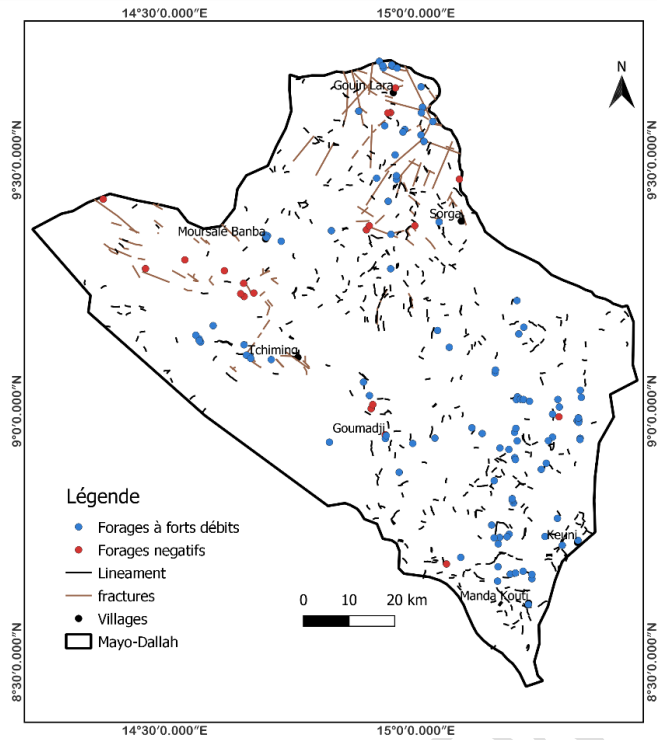
176

Figure 10: Density map of lineaments

177

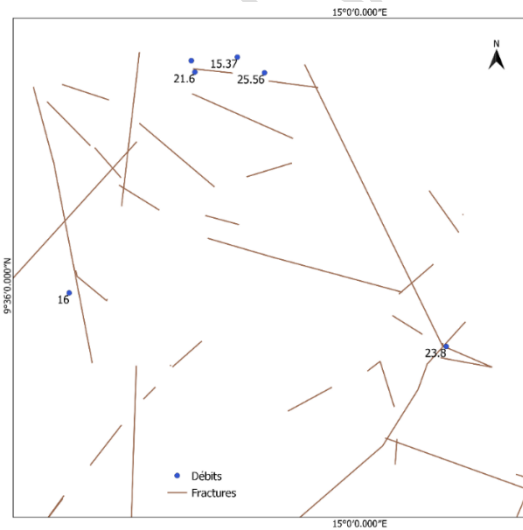
## 6- Relationship between lineaments and borehole flow rates

178 (Krishnamurthy et al., 2000), (Sener, 2005) consider lineaments to be the conduits for  
179 groundwater recharge and flow, and their density indicates a high water content. Figure 12  
180 shows the relationship between lineaments and borehole flow rates. Boreholes located near or  
181 at the intersection of two or more fractures capture significant flows. Characteristic fractures  
182 are highly productive. However, the fractures located to the west of the study area did not  
183 yield satisfactory results.



184  
185  
186

Figure 11: Map of major lineaments and flows



187  
188  
189

Figure 12: Fracture and high-flow map

### 3- Discussion

190 The method of automatic lineament extraction through the LINE module was chosen for  
 191 this study in contrast to the visual interpretation method already used in previous studies of  
 192 the study area. The new authors consider the automatic method to be innovative and  
 193 objective. It saves time thanks to its rapid execution (Tam et al., 2004). The work of (Tam et  
 194 al., 2004), (Hung et al., 2005) showed the potential of the LINE module to detect a maximum  
 195 of lineaments for hydrogeological studies. Application of the LINE algorithm extracted 7193  
 196 lineaments with sizes ranging from 0.2 to 3m. (Doumnang, 2006), (Pouclet et al., 2006),

197 (Penaye et al., 2006) have interpreted the lineament assemblages in the Mayo-Kebbi Province  
198 as being related either to the stratification, foliation or schistosity of the rocks, or to their  
199 diaclasses, fracturation, dyke or vein nature. The distribution of lineaments on the directional  
200 rosette shows a homogeneity of lineaments, but the E-W (80-100°) and N-S (170-180°)  
201 directions stand out from the others in terms of number and cumulative length. These  
202 directions are similar to those of the N170° and E-W (70-100°) normal faults mentioned by  
203 (Penaye et al., 2006) in the Mayo-Kebbi basement. These directions are followed by minority  
204 directions. A total of five lineament families emerge: E-W (80-100°), N-S (N0-20°, N160-  
205 170), SE-NW (140-150°), ESE-WNW (110-130°), NE-SW (40-60°). These fracture directions  
206 correspond to the directions of the Pan-African (schistosity and shears) and post-Pan-African  
207 (Cretaceous fault) structures. The NE-SW direction (N40° and N60°) characterizes the  
208 fracture plane of the Mayo-Kebbi greenstone. It is similar to the schistosity directions  
209 highlighted by (Isseini, 2011 ; Mbaguedjé, 2015) in the Goueygoudoum series. The SE-NW  
210 direction is the same as that of the Doba and Bosso normal faults. This direction is more  
211 likely to be “open” and therefore hydrogeologically productive. The ESE-WNW direction is  
212 similar to local shear zone directions and structures appear to control certain flow channels  
213 (Osinowo et al., 2021). The lineament map of the study area shows all fracture directions in  
214 the Mayo-Kebbi basement. However, these lineaments are subject to validation by  
215 hydrographic, geological and hydrogeological data from the study area to confirm their nature  
216 and existence in the field. The validation of lineaments by the hydrographic network is the  
217 very first validation method used by previous authors. The result shows that the lineaments  
218 are drawn on the watercourses. This result seems logical since, according to (Vidal et al.,  
219 2007), the morphology of Mayo-Kebbi streams is imposed by faults. Fractures guide the path  
220 of rivers and allow lakes to settle in the Mayo-Kebbi Province. Further validation of the  
221 lineaments with the geological and fracture maps of Mayo-Kebbi shows that the majority of  
222 the lineaments are superimposed on the fractures observed in the field. In view of this result,  
223 we can confirm the reliability of the method used and attribute the fracture values to the  
224 lineaments. The density map shows that the south and west have a good density of lineaments.  
225 From a hydrogeological point of view, good fracture densities provide a good understanding  
226 of the aquifer. These zones have a high water potential and influence recharge (Mabee, 2002).  
227 The coupling of drilling points and fractures shows that there is a relationship between  
228 productivity and fracture interconnectivity. Boreholes located at fracture intersections or close  
229 to kilometre-scale fractures capture significant flows, up to 25m<sup>3</sup>/s. This hypothesis has been  
230 validated by (Biemi et al., 1991), (Savané, 1997), Jourda et al., 2006). However, not all  
231 fractures are fed. They may be clogged. This is the case for the boreholes located near the  
232 fractures to the west of the study area. In fact, these fractures run in the same direction as the  
233 old E-W faults. The old faults are likely to be clogged or vein-filled. The relationship between  
234 depth and flow is not significant. It would be important to establish the relationship between  
235 alteration depth (thickness) and flow rate to gain more information.

236

237

#### 4- Conclusion

238 The remote sensing tool has made it possible to map the lineaments in the Mayo-  
239 Dallah Department and has demonstrated their hydrogeological interest. This study leads to  
240 the conclusion that lineaments alone do not guarantee the identification of an aquifer

241 potential. It would be advisable to combine lineaments with other approaches to obtain more  
242 detailed information.

243

244

## 245 **Reference**

246 Biemi, J., Deslandes, S., Gwyn, Q. H. J., et Jourda, P (1991) : Influence des linéaments sur la  
247 productivité des forages dans le bassin versant de Ta Haute Marahoué (Côte d'Ivoire) :  
248 Apport de la télédétection et d'un système d'information à référence spatiale. Télédétection  
249 Gest. Ressour., vol. 7, p. 41-49.

250 Doumnang, Mbaigane, J-C (2006) : Géologie des formations néoproterozoïques du Mayo  
251 Kebbi (Sud-Ouest du Tchad) : apport de la pétrologie et de la géochimie : implications sur la  
252 géodynamique au Panafricain. These de doctorat, Orléans. Consulté le : 1 octobre 2024. [En  
253 ligne]. Disponible sur : <https://theses.fr/2006ORLE2062>.

254 Doumnang, M. J-C., Mbaguedjé, D., Abbas, S. A., Paul, V. J et Roland, G (2021) : Uranium  
255 And Thorium Concentration In Neoproterozoic Formations And Sediments From The Pala  
256 Region Of Mayo-Kebbi, Southwestern Chad. vol. 8, n° 11, 7p

257 Durand, L (2003) : Hydraulique villageoise : Schéma Directeur de l'Eau et de  
258 l'Assainissement du Tchad. 108p.

259 Gleeson, T et Novakowski, K. (2000) : Identifying watershed-scale barriers to groundwater  
260 flow : Lineaments in the Canadian Shield. GSA Bull. vol. 121, n° 3-4, p. 333-347, doi:  
261 10.1130/B26241.1.

262 Hung, L. Q., Batelaan, O et De Smedt, F (2005) : Lineament extraction and analysis,  
263 comparison of LANDSAT ETM and ASTER imagery. Case study : Suoimuoi tropical karst  
264 catchment, Vietnam, in Remote sensing for environmental monitoring, GIS applications, and  
265 geology V, SPIE, p. 182-193. Consulté le : 2 octobre 2024. [En ligne]. Disponible sur :  
266 [https://www.spiedigitallibrary.org/conference-proceedings-of-spie/5983/59830T/Lineament-](https://www.spiedigitallibrary.org/conference-proceedings-of-spie/5983/59830T/Lineament-extraction-and-analysis-comparison-of-LANDSAT-ETM-and-ASTER/10.1117/12.627699.short)  
267 [extraction-and-analysis-comparison-of-LANDSAT-ETM-and-](https://www.spiedigitallibrary.org/conference-proceedings-of-spie/5983/59830T/Lineament-extraction-and-analysis-comparison-of-LANDSAT-ETM-and-ASTER/10.1117/12.627699.short)  
268 [ASTER/10.1117/12.627699.short](https://www.spiedigitallibrary.org/conference-proceedings-of-spie/5983/59830T/Lineament-extraction-and-analysis-comparison-of-LANDSAT-ETM-and-ASTER/10.1117/12.627699.short).

269 Isseini, M (2011) : Crustal Growth and Differentiation during the Neoproterozoic Example of  
270 the Pan-African Domain of Mayo Kebbi in Southwestern Chad. Unpubl. Ph Thesis Univ.  
271 Henri Poincaré Nancy Fr.

272 Jourda, J. P., Saley, M. B., Djagoua, E. V., Kouamé, K. J., Biémi, J et Razack, M. (2006)  
273 : Utilisation des données ETM+ de Landsat et d'un SIG pour l'évaluation du potentiel en eau  
274 souterraine dans le milieu fissuré précambrien de la région de Korhogo (Nord de la Côte  
275 d'Ivoire) : Approche par analyse multicritère et test de validation, Télédétection, vol. 5, n° 4,  
276 p. 339-357.

277 Koudou, A., Assoma, T.V., Adiaffi, B., Youan Ta, M., Kouame, K.F., Lasm, T (2014) :  
278 Analyses statistique et geostatistique de la fracturation extraite de l'imagerie asar envisat du  
279 sud-est de la côte d'ivoire, Consulté le : 30 septembre 2024. [En ligne]. Disponible sur :  
280 <http://archives.univ-biskra.dz:80/handle/123456789/4200>.

- 281 Lasm, T (2000) : Hydrogéologie des réservoirs fracturés de socle : analyses statistique et  
282 géostatistique de la fracturation et des propriétés hydrauliques ; application à la région des  
283 montagnes de Côte d'Ivoire (domaine archéen) », PhD Thesis, Poitiers, 274p.
- 284 Lie, et Gudmundsson, A. (2002):The importance of hydraulic gradient,lineament trend  
285 proximity to lineaments and surface drainage pattern for yield of groundwater wells on  
286 Askey, West Norway. Norges geologiske undersekelse Bulletin 439,51-60.
- 287 Mabee, S. B., Curry, P. J et Hardcastle, K. C (2002) : Correlation of lineaments to ground  
288 water inflows in a bedrock tunnel, *Groundwater*, vol. 40, n° 1, p. 37-43.
- 289 Mbaguedje, D (2015) : Metallogeny of gold and uranium as part of the growth and  
290 differentiation of the Neoproterozoic crust : the example of Mayo-Kebbi massif (Chad) in the  
291 orogenic belt of Central Africa, Consulté le : 2 octobre 2024. [En ligne]. Disponible sur :  
292 [https://policycommons.net/artifacts/15749909/metallogeny-of-gold-and-uranium-as-part-of-](https://policycommons.net/artifacts/15749909/metallogeny-of-gold-and-uranium-as-part-of-the-growth-and-differentiation-of-the-neoproterozoic-crust/16640768)  
293 [the-growth-and-differentiation-of-the-neoproterozoic-crust/16640768](https://policycommons.net/artifacts/15749909/metallogeny-of-gold-and-uranium-as-part-of-the-growth-and-differentiation-of-the-neoproterozoic-crust/16640768).
- 294 Osinowo, O. O., Gomy, A et Isseini, M (2021) : Mapping hydrothermal alteration mineral  
295 deposits from Landsat 8 satellite data in Pala, Mayo Kebbi Region, Southwestern Chad, *Sci.*  
296 *Afr.*, vol. 11, p. e00687.
- 297 Penaye, J., Kröner, A., Toteu, S. F., Van Schmus, W. R et Doumnang, J.-C (2006) : Evolution  
298 of the Mayo Kebbi region as revealed by zircon dating: An early (ca. 740Ma) Pan-African  
299 magmatic arc in southwestern Chad, *J. Afr. Earth Sci.*, vol. 44, n° 4, p. 530-542, a doi:  
300 10.1016/j.jafrearsci.2005.11.018.
- 301 Pouclet, A., Vidal, M., Doumnang, J.-C., Vicat, J.-P et Tchameni, R (2005) : Neoproterozoic  
302 crustal evolution in Southern Chad : Pan-African ocean basin closing, arc accretion and late-  
303 to post-orogenic granitic intrusion, *J. Afr. Earth Sci.*, vol. 44, n° 4, p. 543-560, doi:  
304 10.1016/j.jafrearsci.2005.11.019.
- 305 Sener, E., Davraz, A et Ozcelik, M (2005) : An integration of GIS and remote sensing in  
306 groundwater investigations : A case study in Burdur. Turkey, *Hydrogeol. J.*, vol. 13, n° 5, p.  
307 826-834, doi : 10.1007/s10040-004-0378-5.
- 308 Savané, I (1997) : Contribution à l'étude géologique et hydrogéologique des aquifères  
309 discontinus du socle cristallin d'Odienné (Nord-Ouest de la Côte d'Ivoire). Apport de la  
310 Télédétection et d'un système d'information hydrogéologique à référence spatiale, Apport  
311 Télédétection D'un Syst. D'information Hydrogéologique Aréférence Spatiale These Dr.  
312 D'État Univ. Cocody Abidj., 386 p.
- 313 Tam, V. T., De Smedt, F., Batelaan, O et Dassargues, A (2004) : Study on the relationship  
314 between lineaments and borehole specific capacity in a fractured and karstified limestone area  
315 in Vietnam », *Hydrogeol. J.*, vol. 12, n° 6, p. 662-673, doi : 10.1007/s10040-004-0329-1.
- 316 Vidal, M., Nontanovanh, M., Devineau, J.-L., Doumnang, J.-C. et Pouclet, A. (2007) :  
317 Substratum géologique et partage des terres dans le sud du Tchad Région des lacs de Léré et  
318 de Tréné et réserve de faune de Binder Nayri, in *Quelles aires protégées pour l'Afrique de*  
319 *l'Ouest? Conservation de la biodiversité et développement*, F. A, S. B, et M. G. A, Éd., in  
320 *Colloques et séminaires.*, IRD Editions, 2007. Consulté le : 2 octobre 2024. [En ligne].  
321 Disponible sur : <https://hal.science/hal-00277153>.

322

323

324

325

326

327

328

UNDER PEER REVIEW IN IJAR